Inorg. Chem. **2003**, *42*, 5023–5032

Facile Preparation and Photophysics of Near-Infrared Luminescent Lanthanide(III) Monoporphyrinate Complexes

Timothy J. Foley, Benjamin S. Harrison, Alison S. Knefely, Khalil A. Abboud, John R. Reynolds, Kirk S. Schanze,* and James M. Boncella*

Department of Chemistry and Center for Macromolecular Science and Engineering, University of Florida, Gainesville, Florida 32611-7200

Received February 26, 2003

The synthesis, characterization, and single crystal X-ray diffraction structures of a series of monoporphyrinate, trivalent lanthanide complexes with the monoanionic ligands hydridotris(1-pyrazolyl)borate (Tp) and (cyclopentadienyl)-tris(diethylphosphinito)cobaltate (L(OEt)) having the general formulas M(TPP)(L) (M = Yb, Tm, Er, Ho, Nd, Pr; TPP = 5,10,15,20-tetraphenylporphyrinate; L = Tp, L(OEt)) are described. The photophysical properties of these complexes are also presented including their absorption, emission, and transient absorption properties.

Introduction

There has been increasing interest in generating near-infrared (NIR) emission from metal complexes through photoluminescence[1] or electroluminescence.[2] Sources of near-infrared emission are of interest for a variety of biological and biomedical applications, including glucose monitoring[3] and immunoassay.[4] Furthermore, there are also potential uses for NIR sources in telecommunications[5] and defense applications.[6] Complexes with lanthanide ions are attractive candidates for such NIR devices because a number of these ions display spectrally bright emission in this region.[7]

The narrow band $f \rightarrow f$ emissions of the lanthanide ions are a decidedly attractive optical property. However, direct excitation of these transitions is difficult due to the low optical cross section of lanthanide ions arising from the forbidden nature of the $4f \rightarrow 4f$ transitions.[8] Since the discovery that energy transfer from the triplet state of an organic ligand can efficiently sensitize the emissive states of lanthanide ions,[9] there has been considerable effort devoted to designing ligands that optimize this energy transfer and thus give efficient lanthanide luminescence. While much of

* To whom correspondence should be addressed. E-mail: kschanze@chem.ufl.edu (K.S.S.); boncella@chem.ufl.edu (J.M.B.).

(1) (a) Werts, M. H. V.; Hofstraat, J. W.; Geurts, F. A. J.; Verhoeven, J. W. *Chem. Phys. Lett.* **1997**, *276*, 196. (b) Wolbers, M. P. O.; van Veggel, F. C. J. M.; Snellink-Ruel, B. H. M.; Hofstraat, J. W.; Geurts, F. A. J.; Reinhoudt, D. N. *J. Chem. Soc., Perkin Trans. 2* **1998**, 2141. (c) Klink, S. I.; Grave, L.; Reinhoudt, D. N.; van Veggel, F. C. J. M.; Werts, M. H. V.; Geurts, F. A. J.; Hofstraat, J. W. *J. Phys. Chem. A* **2000**, *104*, 5457. (d) Werts, M. H. V.; Verhoeven, J. W.; Hofstraat, J. W. *J. Chem. Soc., Perkin Trans. 2* **2000**, 433. (e) Klink, S. I.; Alink, P. O.; Grave, L.; Peters, F. G. A.; Hofstraat, J. W.; Geurts, F.; van Veggel, F. C. J. M. *J. Chem. Soc., Perkin Trans. 2* **2001**, 363. (f) Werts, M. H. V. Ph.D. Thesis, University of Amsterdam, 2000.

(2) (a) Sun, R. G.; Wang, Y. Z.; Zheng, Q. B.; Zhang, H. J.; Epstein, A. J. *J. Appl. Phys.* **2000**, *87*, 7589. (b) Harrison, B. S.; Foley, T. J.; Bouguettaya, M.; Boncella, J. M.; Reynolds, J. R.; Schanze, K. S.; Shim, J.; Holloway, P. H.; Padmanaban, G.; Ramakrishnan, S. *Appl. Phys. Lett.* **2001**, *79*, 3770. (c) Slooff, L. H.; Polman, A.; Cacialli, F.; Friend, R. H.; Hebbink, G. A.; van Veggel, F. C. J. M.; Reinhoudt, D. N. *Appl. Phys. Lett.* **2001**, *78*, 2122. (d) Kawamura, Y.; Wada, Y.; Yanagida, S. *Jpn. J. Appl. Phys., Part 1* **2001**, *40*, 350. (e) Hong, Z. R.; Liang, C. J.; Li, R. G.; Zang, F. X.; Fan, D.; Li, W. L.; Hung, L. S.; Lee, S. T. *Appl. Phys. Lett.* **2001**, *79*, 1942. (f) Edwards, A.; Claude, C.; Sokolik, I.; Chu, T. Y.; Okamoto, Y.; Dorsinville, R. *J. Appl. Phys.* **1997**, *82*, 1841−1846. (g) Kido, J.; Okamoto, Y. *Chem. Rev.* **2002**, *102*, 2357.

(3) (a) Muller, U. A.; Mertes, B.; Fischbacher, C.; Jageman, K. U.; Danzer, K. *Int. J. Artif. Organs* **1997**, *20*, 285. (b) Robinson, M. R.; Eaton, R. P.; Haaland, D. M.; Koepp, G. W.; Thomas, E. V.; Stallard, B. R.; Robinson, P. L. *Clin. Chem.* **1992**, *38*, 1618. (c) Samann, A.; Fischbacher, C.; Jagemann, K. U.; Danzer, K.; Schuler, J.; Papenkordt, L.; Muller, U. A. *Exp. Clin. Endocrinol. Diabetes* **2000**, *108*, 406.

(4) (a) Boyer, A. E.; Lipowska, M.; Zen, J. M.; Patonay, G.; Tsang, V. C. W. *Anal. Lett.* **1992**, *25*, 415. (b) Daneshvar, M. I.; Peralta, J. M.; Casay, G. A.; Narayanan, N.; Evans, L.; Patonay, G.; Strekowski, L. *J. Immunol. Methods* **1999**, *226*, 119.

(5) Horuguchi, M. *Ann. Telecommun.* **1993**, *48*, 356.

(6) Rogalski, A.; Chrzanowski, K. *Opto-Electron. Rev.* **2002**, *10*, 111.

(7) *Handbook on the Physics and Chemistry of Rare Earths*; Gscheider, K. A., Eyering, L., Eds.; North-Holland: New York, 1998; Vol. 25.

(8) (a) Hnatejko, Z.; Klonkowski, A.; Lis, S.; Czarnobaj, K.; Pietraszkiewicz, M.; Elbanowski, M. *Mol. Cryst. Liq. Cryst.* **2000**, *354*, 795. (b) Klonkowski, A. M.; Lis, S.; Hnatejko, Z.; Czarnobaj, K.; Pietraszkiewicz, M.; Elbanowski, M. *J. Alloys Compd.* **2000**, *300*, 55. (c) Wang, M. Z.; Jin, L. P.; Bunzli, J. C. G. *Polyhedron* **1999**, *18*, 1853. (d) Kawa, M.; Frechet, J. M. J. *Chem. Mater.* **1998**, *10*, 286. (e) Piguet, C.; Bunzli, J. C. G.; Bernadellia, G.; Hopfgartner, G.; Williams, A. F. *J. Am. Chem. Soc.* **1993**, *115*, 8197. (f) Alpha, B.; Ballardini, R.; Balzani, V.; Lehn, J. M.; Peranthoner, S.; Sabbatini, N. *Photochem. Photobiol.* **1990**, *52*, 299.

(9) (a) Crosby, G. A.; Alire, R. M.; Whan, R. E. *J. Chem. Phys.* **1961**, *34*, 743. (b) Crosby, G. A.; Whan, R. E.; Freeman, J. J. *J. Phys. Chem.* **1962**, *66*, 2493.

10.1021/ic034217g CCC: $25.00
Published on Web 07/12/2003

the focus has been on improvement of the quantum efficiencies of visible emitters such as Eu^{3+} (red) and Tb^{3+} (green),[2g] recently effort has been directed toward investigating ligands for efficient sensitization of the NIR emitting lanthanides.[1,10]

Porphyrins are promising ligands for efficient energy transfer to NIR emitting lanthanide ions because their intense Soret bands lead to high absorption cross sections and their low energy triplet states can efficiently sensitize the NIR emitting states of the lanthanide ions. While porphyrin complexes of transition metals have been studied extensively,[11] comparatively few studies of lanthanide−porphyrin complexes have been reported.[12] The limited work in this area has been directed toward their use as NMR shift reagents,[13] MRI contrast agents,[14] and agents for photodynamic therapy.[15]

The first reported synthesis of lanthanide monoporphyrinates involved distillation of acetylacetone from a $Ln(acac)_3$ complex in the presence of tetraphenylporphyrin (at 220 °C) to give lanthanide monoporphyrinate acetylacetonate complexes in 10−30% yields.[16] The low yields arise because the complexes hydrolyze during the required chromatographic purification step. This method also limits the choice of anionic axial ligand, because of the manner in which the complexes are produced. The coordinated diketonate can be replaced in subsequent reactions, but high boiling solvents are again required and low isolated yields are typical.[17] Recently, efforts to form lanthanide tetraphenylporphyrin (TPP) and other porphyrin complexes have focused on amine elimination reactions of neutral Ln amides or alkyls with free base porphyrins,[18] or similar reactions between $Li\{Ln[N(SiMe_3)_2]_3Cl\}$ and substituted TPPs.[19]

We have recently communicated the high-yield synthesis of a series of lanthanide(III) chloride tetraphenylporphyrinate (Ln(TPP)Cl) complexes via nucleophilic displacement of chloride ion from anhydrous $LnCl_3$ by the TPP dianion.[20] In this paper, we report a high-yield method for the synthesis of Ln(TPP) complexes, capped with multidentate ligands. These synthetic procedures are readily scalable to produce gram quantities of these materials and thereby provide easy access to a variety of new complexes that are potential NIR lumophores. The structures were confirmed using a combination of X-ray crystallography and NMR spectroscopy. Photophysical characterization results are presented as pertinent to the application of these complexes in NIR emitting LEDs.

Experimental Section

Materials and Reagents. Unless otherwise stated, all syntheses were carried out on a double manifold Schlenk line under an atmosphere of nitrogen, or in a N_2 filled glovebox. Glassware was oven dried prior to use. Methylene chloride, dimethoxyethane, and chloroform were purchased from Fisher Scientific and distilled from the appropriate drying agent.[21] Toluene and pentane were purchased from Aldrich Chemicals and dried by passage through a column of activated alumina. Following dehydration, the solvents were degassed and stored over 4 Å molecular sieves in resealable ampules fitted with Teflon valves. The Ln(TPP)Cl(DME) complexes were synthesized according to the literature procedure[20] and stored in a glovebox. Potassium hydridotris(1-pyrazolyl)borate (KTp)[22] and sodium (cyclopentadienyl)tris(diethylphosphinito)cobaltate(I) (NaL-(OEt))[23] were prepared according to literature procedures, dried under vacuum for ∼3 h, and stored in a glovebox. Elemental analyses were performed by Complete Analysis Laboratories, Inc., of Parsippany, NJ, or the University of Florida Spectroscopic Services.

NdTPP(I)(DME). A round-bottomed flask was charged with $NdI_3(THF)_4$ (0.5 g, 0.615 mmol) and $Li_2TPP(DME)$ (0.499 g, 0.696 mmol) in a drybox. After addition of 40 mL of toluene, the flask was removed from the glovebox, and the purple solution was refluxed under N_2. The progress of the reaction was monitored by UV−vis, and after 4 h of reflux, the Soret band at 415 nm had disappeared and was replaced by one at 425 nm indicating complete metalation of the porphyrin. The solution was filtered via cannula while still hot. The residue was then extracted with $CHCl_3$ which was filtered and combined with the toluene solution. The combined extracts were reduced in volume to *ca*. 10 mL. This solution was then layered with pentane. After 12 h, filtration gave a red/purple solid (0.443 g, 0.455 mmol) in 74% yield. X-ray quality crystals were grown from a concentrated THF solution layered with pentane. Anal. Calcd for $C_{48}H_{38}N_4NdIO_2$: C, 59.19; H, 3.93; N, 5.75. Found: C, 57.28; H, 3.97; N, 5.52. ^1H NMR in CD_2Cl_2: δ 8.95 ($\nu_{1/2}$ = 5.78, 8H, *H*-pyrrole), δ 8.12 ($\nu_{1/2}$ = 17.33, 4H, *o*-C_6H_5 TPP), δ 7.56 ($\nu_{1/2}$ = 19.32, 4H, *m*-C_6H_5 TPP), δ 7.31 ($\nu_{1/2}$ = 5.71, 4H, *p*-C_6H_5 TPP), δ 6.92 ($\nu_{1/2}$ = 19.49, 4H, *m*-C_6H_5 TPP), δ 4.90 ($\nu_{1/2}$ = 18.72, 4H, *o*-C_6H_5 TPP), δ −5.42 ($\nu_{1/2}$ = 217, 5H, *H*-DME).

(10) (a) de Sa, G. F.; Malta, O. L.; Donega, C. D.; Simas, A. M.; Longo, R. L.; Santa-Cruz, P. A.; da Silva, E. F. *Coord. Chem. Rev.* **2000**, *196*, 165. (b) Veiopoulou, C. J.; Lianidou, E. S.; Ioannou, P. C.; Efstathiou, C. E. *Anal. Chim. Acta* **1996**, *335*, 177. (c) Gao, X. C.; Cao, H.; Huang, C. H.; Umitani, S.; Chen, G. Q.; Jiang, P. *Synth. Met.* **1999**, *99*, 127.

(11) *The Porphyrin Handbook. Volume 3, Inorganic, Organometallic and Coordination Chemistry*; Kadish, K. M., Smith, K. M., Guilard, R., Eds.; Academic Press: San Diego, CA, 2000.

(12) (a) Hiroshi, T.; Satoshi, S. *Chem. Rev.* **2002**, *102*, 2389. (b) Wong, W.-K.; Zhang, L.; Wong, W.-T.; Xue, F.; Mak, T. C. W. *J. Chem. Soc., Dalton Trans.* **1999**, 615. (c) Spyroulias, G. A.; Despotopoulos, A.; Raptopoulou, C. P.; Terzis, A.; Coutsoleolos, A. G. *Chem. Commun*. **1997**, 783. (d) Radzki, S.; Giannotti, C. *Inorg. Chim. Acta* **1993**, *205*, 213.

(13) Horrocks, W. D.; Wong, C. P. *J. Am. Chem. Soc*. **1976**, *98*, 7157.

(14) (a) Shahbazi-Gahrouei, D.; Williams, M.; Rizvi, S.; Allen, B. J. *J. Magn. Reson. Imag.* **2001**, *14*, 169. (b) Hofmann, B.; Bogdanov, A.; Marecos, E.; Ebert, W.; Semmler, W.; Weissleder, R. J. *Magn. Reson. Imaging* **1999**, *9*, 336.

(15) (a) Sessler, J. L.; Dow, W. C.; O'Connor, D.; Harriman, A.; Hemmi, G.; Mody, T. D.; Miller, R. A.; Qing, F.; Springs, S.; Woodburn, K.; Young, S. W. *J. Alloys Compd.* **1997**, *249*, 146. (b) Sessler, J. L.; Miller, R. A. *Biochem. Pharm.* **2000**, *59*, 733. (c) Parise, R. A.; Miles, D. R.; Egorin, M. J. *J. Chromatogr., B* **2000**, *749*, 145. (d) Mody, T. D.; Sessler, J. L. *J. Porphyrins Phthalocyanines* **2001**, *5*, 134.

(16) (a) Wong, C. P.; Venteicher, R.; Horrocks, W. D. *J. Am. Chem. Soc.* **1974**, *96*, 7149. (b) Wong, C. P. *Inorg. Synth.* **1983**, *22*, 156.

(17) (a) Spyroulias, G. A.; de Montauzon, D.; Maisonat, A.; Poilblanc, R.; Coutsolelos, A. G. *Inorg. Chem. Acta* **1998**, *276*, 182. (b) Spyroulias, G. A.; Coutsolelos, A. G.; Raptopoulou, C. P.; Terzis, A. *Inorg. Chem.* **1995**, *34*, 2476. (c) Jiang, J. Z.; Mak, T. C. W.; Ng, D. K. P. *Chem. Ber.* **1996**, *129*, 933.

(18) (a) Schaverien, C. J.; Orpen, A. G. *Inorg. Chem.* **1991**, *30*, 4968. (b) Schaverien, C. J. *Chem. Commun.* **1991**, 458.

(19) (a) Wong, W. K.; Zhang, L. L.; Wong, W. T.; Xue, F.; Mak, T. C. W. *J. Chem. Soc., Dalton Trans.* **1999**, 615. (b) Wong, W. K.; Zhang, L.; Xue, F.; Mak, T. C. W. *J. Chem. Soc, Dalton Trans.* **1999**, 3053.

(20) Foley, T. J.; Abboud, K. A.; Boncella, J. M. *Inorg. Chem.* **2002**, *41*, 1704.

(21) Gordon, A. J.; Ford, R. A. *The Chemist's Companion*; Wiley: New York, 1972.

(22) Trofimenko, S. *J. Am. Chem. Soc.* **1967**, *89*, 6288.

(23) Klaui, W.; Dehnicke, K. *Chem. Ber.* **1978**, *111*, 451.

PrTPP(I)(DME). In the same fashion as NdTPPI(DME), PrTPPI(DME) was synthesized by refluxing $PrI_3(THF)_4$ (0.5 g, 0.617 mmol) and Li_2TPP (DME) (0.501 g, 0.699 mmol) in toluene for 4 h. The purple solid was isolated in 74% yield (0.44 g, 0.451 mmol). Anal. Calcd for $C_{48}H_{38}N_4PrIO_2$: C, 59.39; H, 3.95; N, 5.77. Found: C, 58.99; H, 3.96; N, 5.84. ^{1}H NMR in $CDCl_3$: δ 7.73 ($\nu_{1/2}$ = 16.19, 4H, *o*-C_6H_5 Tpp), δ 6.81 ($\nu_{1/2}$ = 18.68, 4H, *m*-C_6H_5 Tpp), δ 6.29 ($\nu_{1/2}$ = 5.07, 4H, *p*-C_6H_5 Tpp), δ 5.53 ($\nu_{1/2}$ = 5.73, 8H, *H*-pyrrole), δ 5.33 ($\nu_{1/2}$ = 18.79, 4H, *m*-C_6H_5 TPP), δ 0.78 ($\nu_{1/2}$ = 17.79, 4H, *o*-C_6H_5 TPP).

Yb(TPP)Tp. A solution of YbTPP(Cl)(DME) (0.300 g, 3.29×10^{-1} mmol) in DME (ca. 65 mL) was stirred vigorously while potassium hydridotris(1-pyrazolyl)borate (KTp) (0.084 g, 3.33×10^{-1} mmol) was added. Following addition, the solution was allowed to stir at room temperature for 12 h. The solvent was then removed *in vacuo*, and the purple residue was extracted with ca. 30 mL of methylene chloride, leaving behind a brown residue. The solution was then filtered, reduced to ca. 10 mL, and layered with ca. 30 mL of pentane. Purple crystals formed on standing overnight. The supernatant was filtered, concentrated, and cooled to −78 °C whereupon an additional amount of product precipitated. The isolated solids were then combined, dissolved in ca. 20 mL of methylene chloride, and cooled to −78 °C. Crystals then formed, which were isolated by cannula filtration giving 0.265 g of product (88%). Single crystals of X-ray diffraction quality were grown by slow evaporation of a benzene solution of Yb(TPP)Tp in an inert atmosphere. Anal. Calcd for $C_{53}H_{38}BN_{10}Yb$: C, 63.73; H, 3.83; N, 14.02. Found: C, 64.23; H, 3.91; N, 13.89. ^{1}H NMR (C_6D_6, 294 K, ppm): 22.71 ($\nu_{1/2}$ = 53.24 Hz, 3H, H-Tp), 15.48 ($\nu_{1/2}$ = 40.81 Hz, 4H, *o*-C_6H_5 TPP), 13.88 ($\nu_{1/2}$ = 25.90, 8H, H-pyrrole), 9.73 ($\nu_{1/2}$ = 39.55 Hz, 4H, *m*-C_6H_5 TPP), 8.77 ($\nu_{1/2}$ = 26.74, 4H, *p*-C_6H_5 TPP), 8.09 ($\nu_{1/2}$ = 43.17 Hz, 4H, *m*-C_6H_5 TPP), 7.83 ($\nu_{1/2}$ = 44.39 Hz, 4H, *o*-C_6H_5 TPP), 4.62 ($\nu_{1/2}$ = 23.34 Hz, 3H, H-Tp), −3.03 ($\nu_{1/2}$ = 23.81 Hz, 3H, H-Tp).

Tm(TPP)Tp. The procedure used to generate this complex was the same as that used for Yb(TPP)Tp with TmTPP(Cl)(DME) (0.300 g, 3.33×10^{-1} mmol) and KTp (0.084 g, 3.33×10^{-1} mmol) reacting to give 0.244 g of Tm(TPP)Tp (81%). X-ray diffraction quality single crystals of Tm(TPP)Tp were obtained by slow evaporation of a chloroform solution under an inert atmosphere. Anal. Calcd for $C_{53}H_{38}BN_{10}Tm$: C, 64.00; H, 3.85; N, 14.08. Found: C, 64.52; H, 3.83; N, 14.11. ^{1}H NMR (C_6D_6, 294 K, ppm): 122.96 (113.08 Hz, 3H, H-Tp), 55.33 (58.73 Hz, 4H, *o*-C_6H_5 TPP), 38.92 ($\nu_{1/2}$ = 38.16 Hz, 8H, H-pyrrole), 22.81 ($\nu_{1/2}$ = 31.80 Hz, 4H, *m*-C_6H_5 TPP), 16.11 ($\nu_{1/2}$ = 22.84 Hz, 4H, *p*-C_6H_5 TPP), 11.97 ($\nu_{1/2}$ = 30.49 Hz, 4H, *m*-C_6H_5 TPP), 7.28 ($\nu_{1/2}$ = 79.37 Hz, 3H, H-Tp), 3.72 ($\nu_{1/2}$ = 25.72 Hz, 3H, H-Tp), −55.91 ($\nu_{1/2}$ = 30.92 Hz, 4H, *o*-C_6H_5 TPP).

Er(TPP)Tp. The procedure used to generate this complex was the same as that used for Yb(TPP)Tp with ErTPP(Cl)(DME) (0.300 g, 3.33×10^{-1} mmol) and KTp (0.084 g, 3.33×10^{-1} mmol) reacting to give 0.271 g of Er(TPP)Tp (90%). Anal. Calcd for $C_{53}H_{38}BN_{10}Er$: C, 64.10; H, 3.86; N, 14.11. Found: C, 63.85; H, 3.12; N, 14.69. ^{1}H NMR (C_6D_6, 294 K, ppm): 61.76 ($\nu_{1/2}$ = 493.43 Hz, 3H, H-Tp), 32.13 ($\nu_{1/2}$ = 94.73 Hz, 4H, *o*-C_6H_5 TPP), 20.90 ($\nu_{1/2}$ = 72.68 Hz, 8H, H-pyrrole), 15.14 ($\nu_{1/2}$ = 30.38 Hz, 4H, *m*-C_6H_5 TPP), 11.84 ($\nu_{1/2}$ = 18.77 Hz, 4H, *p*-C_6H_5 TPP), 9.63 ($\nu_{1/2}$ = 28.32 Hz, 4H, *m*-C_6H_5 TPP), 7.66 ($\nu_{1/2}$ = 55.83 Hz, 4H, *o*-C_6H_5 TPP), 2.82 ($\nu_{1/2}$ = 48.22 Hz, 3H, H-Tp), −24.79 ($\nu_{1/2}$ = 59.67 Hz, 3H, H-Tp).

Ho(TPP)Tp. The procedure used to generate this complex was the same as that used for Yb(TPP)Tp with HoTPP(Cl)(DME) (0.300 g, 3.32×10^{-1} mmol) and KTp (0.084 g, 3.33×10^{-1} mmol) reacting to give 0.255 g of Ho(TPP)Tp (85%). Anal. Calcd for $C_{53}H_{38}BN_{10}Ho$: C, 64.26; H, 3.87; N, 14.14. Found: C, 63.75; H, 3.77; N, 13.75. ^{1}H NMR (C_6D_6, 294 K, ppm): 40.30 ($\nu_{1/2}$ = 139.20 Hz, 3H, H-Tp), 8.90 ($\nu_{1/2}$ = 84.74 Hz, 4H, *o*-C_6H_5 TPP), 4.62 ($\nu_{1/2}$ = 40.08 Hz, 4H, *m*-C_6H_5 TPP), 3.11 ($\nu_{1/2}$ = 95.88 Hz, 3H, H-Tp), 2.43 ($\nu_{1/2}$ = 26.86 Hz, 4H, *p*-C_6H_5 TPP), 1.36 ($\nu_{1/2}$ = 38.59 Hz, 3H, H-Tp), −1.90 ($\nu_{1/2}$ = 43.16 Hz, 4H, *m*-C_6H_5 TPP), −14.98 ($\nu_{1/2}$ = 113.24 Hz, 8H, H-pyrrole), −19.90 ($\nu_{1/2}$ = 121.76 Hz, 4H, *o*-C_6H_5 TPP).

Nd(TPP)Tp. To a stirred solution of NdTPP(I)(DME) (0.152 g, 0.16 mmol) in DME was added KTp (0.041 g, 0.16 mmol). The solution was stirred for an additional 12 h at room temperature. The solvent was then removed *in vacuo*, and the residue was extracted with approximately 30 mL of CH_2Cl_2, leaving a white, insoluble solid. The volume of the red/purple solution was then reduced to 10 mL and layered with pentane. After being cooled to −10 °C for 12 h, the solution was filtered, leaving a crystalline, purple solid. The filtrate was then concentrated and cooled to −10 °C affording a second crop of crystals. Recrystallization of the combined solids from CH_2Cl_2/pentane gave X-ray quality crystals of Nd(TPP)Tp in 64% yield (0.093 g, 0.0962 mmol). Anal. Calcd for $C_{53}H_{38}BN_{10}Nd$: C, 65.27; H, 3.95; N, 14.44. Found: C, 65.67; H, 3.96; N, 14.33. ^{1}H NMR (C_6D_6, 294 K, ppm): 14.65 ($\nu_{1/2}$ = 5.61 Hz, 3H, *H*-Tp), 7.97 ($\nu_{1/2}$ = 15.05 Hz, 4H, *o*-C_6H_5 TPP), 7.82 ($\nu_{1/2}$ = 4.25 Hz, 8H, *H*-pyrrole), 6.93 ($\nu_{1/2}$ = 5.08 Hz, 7H, *m*-C_6H_5 TPP, *H*-Tp), 6.47 ($\nu_{1/2}$ = 3.25 Hz, 4H, *p*-C_6H_5 TPP), 5.75 ($\nu_{1/2}$ = 16.88 Hz, 4H, *m*-C_6H_5 TPP), 2.88 ($\nu_{1/2}$ = 15.66 Hz, 4H, *o*-C_6H_5 TPP), −6.23 ($\nu_{1/2}$ = 22.41 Hz, 3H, *H*-Tp).

Pr(TPP)Tp. Following the procedure used to generate Nd(TPP)Tp, PrTPP(I)(DME) (0.160 g, 0.155 mmol) and KTp(0.041 g, 0.16 mmol) were combined together in dry DME and allowed to react for 12 h. After recrystallization, 0.073 g of Pr(TPP)Tp was collected (0.076 mmol, 49%). Anal. Calcd for $C_{53}H_{38}BN_{10}Pr$: C, 65.85; H, 3.96; N, 14.49. Found: C, 66.30; H, 3.91; N, 14.23. ^{1}H NMR (C_6D_6, 294 K, ppm): 18.08 ($\nu_{1/2}$ = 4.89 Hz, 3H, *H*-Tp), 8.13 ($\nu_{1/2}$ = 14.81 Hz, 4H, *o*-C_6H_5 TPP), 6.63 ($\nu_{1/2}$ = 5.09 Hz, 7H, *m*-C_6H_5 TPP, *H*-Tp), 5.90 ($\nu_{1/2}$ = 3.97 Hz, 4H, *p*-C_6H_5 TPP), 5.36 ($\nu_{1/2}$ = 3.69 Hz, 8H, *H*-pyrrole), 4.64 ($\nu_{1/2}$ = 17.51 Hz, 4H, *m*-C_6H_5 TPP), −0.47 ($\nu_{1/2}$ = 14.09 Hz, 4H, *o*-C_6H_5 TPP), −13.87 ($\nu_{1/2}$ = 11.23 Hz, 3H, *H*-Tp).

Yb(TPP)(L(OEt)). A solution of YbTPP(Cl)(DME) (0.150 g, 1.65×10^{-1} mmol) in DME (ca.50 mL) was stirred vigorously while solid sodium (cyclopentadienyl)tris(diethylphosphinito)-cobaltate(I) (NaL(OEt)) (0.088 g, 1.57×10^{-1} mmol) was added. The solution was then stirred at room temperature for 12 h, after which time the DME was removed in vacuo leaving a purple, amorphous solid. The solid was extracted twice with ca. 15 mL of toluene, leaving behind a slight amount of brown residue. The two extracts were filtered, combined, and reduced to ca. 10 mL to which was added ca. 30 mL of pentane producing a small amount of brown precipitate. The solution was filtered to remove the precipitate and then cooled to −78 °C. Purple crystals of the product formed on standing for 5 h and were isolated via cannula filtration. Residual solvents were removed from the crystals in vacuo, giving 0.200 g of product (96%). Anal. Calcd for $C_{61}H_{65}CoN_4O_9P_3Yb$: C, 55.46; H, 4.91; N, 4.20. Found: C, 55.40; H, 4.95; N, 4.23. ^{1}H NMR (C_6D_6, 294 K, ppm): 17.41 ($\nu_{1/2}$ = 18.27 Hz, 4H, *o*-C_6H_5 TPP), 15.81 ($\nu_{1/2}$ = 8.22, 8H, H-pyrrole), 10.68 ($\nu_{1/2}$ = 8.03 Hz, 4H, *m*-C_6H_5 TPP), 9.40 ($\nu_{1/2}$ = 4.43 Hz, 7 Hz, 4H, *p*-C_6H_5 TPP), 8.91 ($\nu_{1/2}$ = 17.09 Hz, 6H, OCH_2CH_3), 8.63 ($\nu_{1/2}$ = 18.20 Hz, 4H, *o*-C_6H_5 TPP), 8.45 ($\nu_{1/2}$ = 28.34 Hz, 4H, *m*-C_6H_5 TPP), 7.67 ($\nu_{1/2}$= 29.31 Hz, 6H, OCH_2CH_3), 3.05 ($\nu_{1/2}$ = 10.45 Hz, 18H, OCH_2CH_3), −4.67($\nu_{1/2}$ = 4.10 Hz, 5H, Cp*H*).

Tm(TPP)(L(OEt)). The synthetic procedure used was the same as that used for Yb(TPP)L(OEt) with TmTPP(Cl)(DME) (0.150 g, 1.65×10^{-4} mol) reacting with Na(L(OEt)) (0.088 g, 1.57×10^{-1} mmol) to give 0.133 g of Tm(TPP)(L(OEt)) (64%). Anal. Calcd for $C_{61}H_{65}CoN_4O_9P_3Tm$: C, 55.63; H, 4.82; N, 4.25. Found: C, 51.92; H, 5.45; N, 3.37. ^{1}H NMR (C_6D_6, 294 K, ppm): 67.59 ($\nu_{1/2}$ = 49.68 Hz, 4H, *o*-C_6H_5 TPP), 52.41 ($\nu_{1/2}$ = 34.64 Hz, 8H, H-pyrrole), 40.92 ($\nu_{1/2}$ = 70.14 Hz, 6H, OC*H*$_2$CH$_3$), 35.49 ($\nu_{1/2}$ = 74.76 Hz, 6H, OC*H*$_2$CH$_3$), 27.22 ($\nu_{1/2}$ = 21.01 Hz, 4H, *m*-C_6H_5 TPP), 18.95 ($\nu_{1/2}$ = 19.63 Hz, 4H, *p*-C_6H_5 TPP), 14.72 ($\nu_{1/2}$ = 21.20 Hz, 5H, Cp*H*), 14.52 ($\nu_{1/2}$ = 14.77 Hz, 18H, OCH$_2$C*H*$_3$), 11.58 ($\nu_{1/2}$ = 23.59 Hz, 4H, *m*-C_6H_5 TPP), −55.78 ($\nu_{1/2}$ = 14.47 Hz, 4H, *o*-C_6H_5 TPP).

Er(TPP)(L(OEt)). The synthetic procedure was the same as that used for Yb(TPP)(L(OEt)) with ErTPP(Cl)(DME) (0.150 g, 1.65×10^{-1} mmol) reacting with Na(L(OEt)) (0.088 g, 1.57×10^{-1} mmol) to give 0.155 g of Er(TPP)(L(OEt)) (75%). Anal. Calcd for $C_{61}H_{65}CoN_4O_9P_3Er$: C, 55.71; H, 4.83; N, 4.26. Found: C, 56.04; H, 4.84; N, 4.08. ^{1}H NMR (C_6D_6, 294 K, ppm): 46.29 ($\nu_{1/2}$ = 82.29 Hz, 4H, *o*-C_6H_5 TPP), 34.74 ($\nu_{1/2}$ = 77.14 Hz, 8H, H-pyrrole), 27.39 ($\nu_{1/2}$ = 170.34 Hz, 6H, OC*H*$_2$CH$_3$), 23.10 ($\nu_{1/2}$ = 185.68 Hz, 6H, OC*H*$_2$CH$_3$), 20.08 ($\nu_{1/2}$ = 22.69 Hz, 4H, *m*-C_6H_5 TPP), 14.73 ($\nu_{1/2}$ = 16.91 Hz, 4H, *p*-C_6H_5 TPP), 11.92 ($\nu_{1/2}$ = 20.65 Hz, 4H, *m*-C_6H_5 TPP), 10.23 ($\nu_{1/2}$ = 52.65 Hz, 5H, Cp*H*), 9.71 ($\nu_{1/2}$ = 32.28 Hz, 18H, OCH$_2$C*H*$_3$), −34.72 ($\nu_{1/2}$ = 21.95 Hz, 4H, *o*-C_6H_5 TPP).

Ho(TPP)(L(OEt)). The synthetic procedure was the same as that used for Yb(TPP)(L(OEt)), substituting HoTPP(Cl)(DME) (0.150 g, 1.66×10^{-1} mmol) and allowing it to react with Na(L(OEt)) (0.088 g, 1.57×10^{-1} mmol) to give 0.146 g of Ho(TPP)(L(OEt)) (71%). Anal. Calcd for $C_{61}H_{65}CoN_4O_9P_3Ho$: C, 55.80; H, 4.84; N, 4.26. Found: C, 55.67; H, 4.46; N, 4.65. ^{1}H NMR (C_6D_6, 294 K, ppm): 40.39 ($\nu_{1/2}$ = 65.17 Hz, 4H, *o*-C_6H_5 TPP), 6.77 ($\nu_{1/2}$ = 90.51 Hz, 5H, Cp*H*), 3.10 ($\nu_{1/2}$ = 28.32 Hz, 4H, *m*-C_6H_5 TPP), 0.61 ($\nu_{1/2}$ = 16.20 Hz, 4H, *p*-C_6H_5 TPP), −4.63 ($\nu_{1/2}$ = 29.23 Hz, 4H, *m*-C_6H_5 TPP), −7.98 ($\nu_{1/2}$ = 60.87 Hz, 18H, OCH$_2$C*H*$_3$), −17.77 ($\nu_{1/2}$ = 478.58 Hz, 12 H, OC*H*$_2$CH$_3$), −20.81 ($\nu_{1/2}$ = 125.81 Hz, 8H, H-pyrrole), −28.52 ($\nu_{1/2}$ = 138.57 Hz, 4H, *o*-C_6H_5 TPP).

Nd(TPP)(L(OEt)). To a stirred solution of NdTPP(I)(DME) (0.125 g, 0.128 mmol) in THF was added 0.075 g of K(L(OEt)) (0.125 mmol). The purple solution was stirred for 12 h at room temperature. The solvent was then removed in vacuo, and the product was extracted with 30 mL of toluene which was filtered, concentrated to ca. 10 mL, and layered with pentane. After cooling to −78 °C for 24 h, the purple precipitate was isolated by filtration and recrystallized from CH_2Cl_2/pentane. The crystals were washed with pentane to give 30% (0.05 g, 0.039 mmol). Anal. Calcd for $C_{61}H_{63}CoN_4O_9P_3Nd$: C, 56.70; N, 4.34; H, 4.91. Found: C, 55.13; N, 3.81; H, 4.81. ^{1}H NMR (C_6D_6, 294 K, ppm): 10.13 ($\nu_{1/2}$ = 3.28 Hz, 5H, *H*-Cp), 7.98 ($\nu_{1/2}$ = 19.35 Hz, 4H, *o*-C_6H_5 TPP), 6.80 ($\nu_{1/2}$ = 20.88 Hz, 4H, *m*-C_6H_5 TPP), 6.53 ($\nu_{1/2}$ = 4.32 Hz, 8H, *H*-pyrrole), 6.35 ($\nu_{1/2}$ = 3.22 Hz, 4H, *p*-C_6H_5 TPP), 5.61 ($\nu_{1/2}$ = 20.32 Hz, 4H, *m*-C_6H_5 TPP), 2.02 ($\nu_{1/2}$ = 20.63 Hz, 4H, *o*-C_6H_5 TPP), −0.26 ($\nu_{1/2}$ = 47.23 Hz, 12H, −OC*H*$_2$CH$_3$), −0.83 ($\nu_{1/2}$ = 11.27, 18H, OCH$_2$C*H*$_3$).

Pr(TPP)(L(OEt)). The procedure developed for the synthesis of Nd(TPP)(L(OEt)) was used to prepare Pr(TPP)(L(OEt)), from PrTPP(I)(DME) (0.2 g, 0.206 mmol) and K(L(OEt)) (0.121 g, 0.206 mmol) giving 0.08 g of the complex (30%, 0.062 mmol). Anal. Calcd for $C_{61}H_{53}CoN_4O_9P_3Pr$: C, 56.84; N, 4.35; H, 4.93. Found: C, 55.73; N, 3.84; H, 4.96. ^{1}H NMR (C_6D_6, 294 K, ppm): 14.92 ($\nu_{1/2}$ = 1.79 Hz, 5H, *H*-Cp), 7.96 ($\nu_{1/2}$ = 23.50 Hz, 4H, *o*-C_6H_5 TPP), 6.28 ($\nu_{1/2}$ = 26.26 Hz, 4H, *m*-C_6H_5 TPP), 5.45 ($\nu_{1/2}$ = 3.21 Hz, 4H, *p*-C_6H_5 TPP), 3.96 ($\nu_{1/2}$ = 26.20 Hz, 4H, *m*-C_6H_5 TPP), 3.04 ($\nu_{1/2}$ = 2.47 Hz, 8H, *H*-pyrrole), −2.16 ($\nu_{1/2}$ = 13.98 Hz, 18H, −OCH$_2$C*H*$_3$), −2.39 ($\nu_{1/2}$ = 30.25 Hz, 6H, −OC*H*$_2$CH$_3$), −2.59 ($\nu_{1/2}$ = 27.79 Hz, 6H, −OC*H*$_2$CH$_3$), −3.02 ($\nu_{1/2}$ = 25.20 Hz, 4H, *o*-C_6H_5 TPP).

X-ray Crystallographic Measurements. Data were collected at 173 K on a Siemens SMART PLATFORM equipped with a CCD area detector and a graphite monochromator utilizing Mo Kα radiation (λ = 0.71073 Å). Cell parameters were refined using up to 8192 reflections. A full sphere of data (1850 frames) was collected using the ω-scan method (0.3° frame width). The first 50 frames were remeasured at the end of data collection to monitor instrument and crystal stability (maximum correction on *I* was <1%). Absorption corrections by integration were applied on the basis of measured indexed crystal faces. All structures were solved by direct methods in *SHELXTL5*[24] and refined using full-matrix least-squares. The non-H atoms were treated anisotropically, whereas the hydrogen atoms were calculated in ideal positions and were riding on their respective carbon atoms, except the boron H atom which was obtained from a difference Fourier map and refined freely.

For the structure of Nd(TPP)I(THF)$_2$, the asymmetric unit consists of the complex and a disordered THF molecule. The THF molecule could not be modeled properly; thus, program SQUEEZE, a part of the PLATON package of crystallographic software, was used to calculate the solvent disorder area and remove its contribution to the overall intensity data. The complex has its iodine and two THF ligands disordered about a 2-fold rotation axis perpendicular to the plane of the macrocycle, but only the iodine atom of the minor part could be seen due to its small site occupation factor (refined to 5% then fixed in the final cycles of refinement). A total of 548 parameters were refined in the final cycle of refinement using 21110 reflections with $I > 2\sigma(I)$ to yield R1 and wR2 values of 4.06% and 10.31%, respectively. Refinement was done using F^2.

For the structure of Yb(TPP)Tp, the asymmetric unit consists of the complex and four benzene molecules. Two of the solvent molecules were disordered in their respective planes, and each was refined in two parts. The site occupation factors of the minor and major parts in each disordered molecule were dependently refined to 0.54(2) and 0.53(1) for the C80 and the C90 benzene molecules major parts, respectively. The disordered molecules were restrained to maintain equivalent geometries throughout the refinement, and their C atoms were refined with isotropic thermal parameters. A total of 797 parameters were refined in the final cycle of refinement using 12598 reflections with $I > 2\sigma(I)$ to yield R1 and wR2 values of 2.69% and 6.50%, respectively. Refinement was done using F^2.

For the structure of Tm(TPP)Tp, the asymmetric unit consists of the Tm complex and two chloroform molecules of crystallization. A total of 663 parameters were refined in the final cycle of refinement using 10920 reflections with $I > 2\sigma(I)$ to yield R1 and wR2 values of 3.40% and 7.28%, respectively. Refinement was done using F^2.

For the structure of Nd(TPP)Tp, the asymmetric unit consists of two complexes and a pentane molecule disordered over a center of inversion site. The disorder is resolved where only the methyl groups are disordered. A total of 1208 parameters were refined in the final cycle of refinement using 12451 reflections with $I > 2\sigma(I)$ to yield R1 and wR2 of 3.69% and 6.42%, respectively. Refinement was done using F^2.

Nuclear Magnetic Resonance Spectroscopy. Spectra were recorded in 5 mm Kontes resealable NMR tubes. Proton NMR

(24) Sheldrick, G. M. *SHELXTL5*; Bruker-AXS: Madison, WI, 1998.

Scheme 1

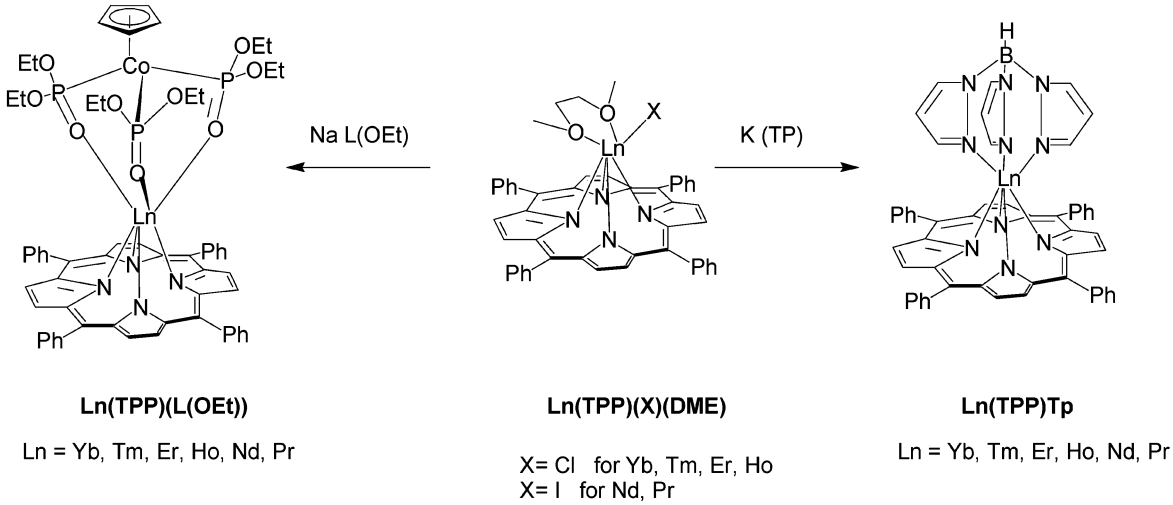

spectra were measured at 300 MHz on a Varian Gemini 300, VXR 300, or Mercury 300 with C_6D_6 as the solvent unless otherwise noted. Chemical shifts in the spectra were referenced to the residual protons on the deuterated solvent and are reported in parts per million downfield from tetramethylsilane ($\delta = 0$). For paramagnetic complexes, the acquisition times were varied according to the relaxation rate enhancement provided by the lanthanide, and the spectral window width was determined by expanding the window of the spectrum until the peak positions remained invariant to further expansions. The number of transients collected for an individual spectrum varied with the nature of the metal, with the minimum being determined by the noise in the particular spectrum. COSY spectra were collected using the standard parameters that accompanied the Varian operating software.

Photophysical Measurements. All photophysical studies were conducted in 1 cm^2 quartz cuvettes unless otherwise noted. All absorption, emission, and lifetime measurements were made in CH_2Cl_2 unless otherwise noted. Absorption spectra were obtained on a double-beam Cary-100 UV−vis spectrometer. Fluorescence spectra were measured on a SPEX Fluorolog-2 equipped with a thermoelectric-cooled PMT detector or on a spectrometer consisting of an ISA-SPEX Triax 180 spectrograph equipped with a liquid N_2 cooled CCD detector (Hamamatsu CCD, 1024 × 64 pixel, 400−1100 nm). Near-IR measurements were measured on a SPEX Fluorolog-2 equipped with a liquid N_2 cooled InGaAs detector (800−1600 nm). All measurements were corrected for detector response. Emission quantum yields were measured by relative actinometry with H_2TPP ($\phi = 0.11$) or ZnTPP ($\phi = 0.033$). Near-IR quantum yields were determined for Yb(TPP)Tp and Yb(TPP)(L(OEt)) on the CCD fluorescence system using the visible H_2TPP and ZnTPP actinometers. Then, the emission quantum yields for the Nd and Er complexes were determined relative to Yb(TPP)Tp using the SPEX Fluorolog-2 with the InGaAs detector.

Time-resolved emission decays were obtained by time-correlated single photon counting on an instrument that was constructed in-house. Excitation was effected by using either a pulsed LED source or a blue-pulsed diode laser (IBH instruments, Edinburgh, Scotland). The pulsed LED and diode laser sources have pulse widths of ca. 1 ns. Time-resolved emission was collected using a red sensitive, photon-counting PMT (Hamamatsu R928), and the light was filtered using 10 nm band-pass interference filters. Lifetimes were determined from the observed decays by using fluorescence lifetime deconvolution software. Nanosecond transient absorption spectra measurements were obtained on previously described instrumentation,[25] with the third harmonic of a Nd:YAG laser (355 nm, 10 ns fwhm, 5 mJ $pulse^{-1}$) as the excitation source. Samples were thoroughly degassed with argon. Primary factor analysis followed by first order (A → B) least-squares fits of the transient absorption data was accomplished with SPECFIT global analysis software (Spectrum Software Associates).

Results and Discussion

Synthesis and Structural Characterization. The synthesis of the Ln(TPP)Tp and Ln(TPP)(L(OEt)) complexes involved reaction of LnTPP(X)(DME) with the Tp or (L(OEt)) anions under anhydrous, oxygen-free conditions as summarized in Scheme 1. We believed that, by replacement of the halide and DME ligands with a multidentate, monoanionic ligand, the increased steric bulk around the lanthanide complex would minimize interactions between the metal and quenching agents and thereby enhance the photoluminescence yields in the NIR. This synthesis is somewhat different from that of other Ln porphyrins found in the literature because the complexes are always handled under inert atmosphere and the procedure avoids the use of column chromatography for purification. The use of recrystallization facilitates the preparation of large quantities of these complexes, and the reactions have been performed successfully on a 1-g scale with no loss in yield or purity. While column chromatography is useful for the purification of LnTPP complexes, the hydrolytic instability of the Ln−N bonds leads to decomposition on the column giving dramatically reduced isolated yields.

These complexes are stable in air in the solid state over the course of several days, but we have observed that demetalation of the porphyrin ligands becomes noticeable over an extended period of time. Thus, the NIR photoluminescence intensity decreases and the visible fluorescence from free porphyrin impurities increases when the samples are stored in air for several weeks, while samples which are stored under an inert atmosphere have consistent NIR emission intensities and weak or unobservable free porphyrin emission. The degradation of these compounds over time is

(25) Wang, Y. S.; Schanze, K. S. *Chem. Phys.* **1993**, *176*, 305.

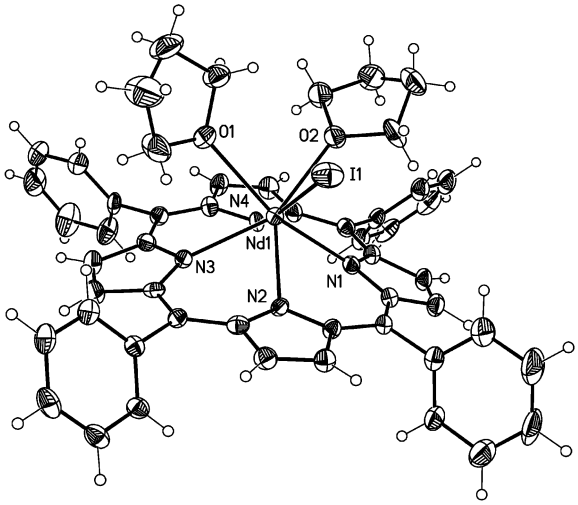

Figure 1. Thermal ellipsoid plot of the molecular structure of Nd(TPP)(I)(THF)$_2$showing selected atom labels. All thermal ellipsoids are drawn at the 50% probability level; all hydrogen atoms and solvent atoms in the crystal structure have been omitted for clarity.

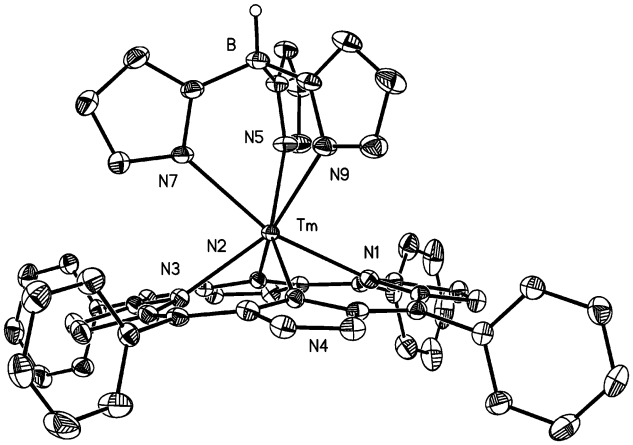

Figure 2. Thermal ellipsoid plot of the molecular structure of Tm(TPP)Tp showing selected atom labels. All thermal ellipsoids are drawn at the 50% probability level; all hydrogens and two molecules of chloroform have been excluded for clarity. Nonlabeled atoms are carbon.

consistent with the slow hydrolysis of the Ln−N_{TPP} bonds under ambient conditions.[26] Therefore, to maximize the shelf life of these compounds, it is necessary that they be stored in an anhydrous, oxygen free environment.

X-ray Crystallography. Single crystals of Nd(TPP)(I)(THF)$_2$, Yb(TPP)(Tp), Tm(TPP)(Tp), and Nd(TPP)(Tp) were obtained as described in the Experimental Section. Thermal ellipsoid plots of Nd(TPP)(I)(THF)$_2$ and Tm(TPP)(Tp) are shown in Figures 1 and 2 while the crystal data and data collection parameters for all four complexes are found in Table 1. Solvent(s) of crystallization have been omitted from Figures 1 and 2 for clarity. In general, all the structures share the common feature that the metal ions are too large to fit in the cavity of the porphyrin ring and sit above the plane defined by the four N atoms of the porphyrin with the remaining ligands completing the coordination sphere of the metal. The coordination geometry of the metal centers is best described as distorted capped trigonal prisms with the trigonal

(26) Haye, S.; Hambright, P. *Chem. Commun.* **1988**, 666.

Table 1. Crystal Data for Complexes

	Nd(TPP)(I)(THF)$_2$	Yb(TPP)Tp	Tm(TPP)Tp	Nd(TPP)Tp
empirical formula	$C_{56}H_{52}IN_4NdO_3$	$C_{77}H_{62}BN_{10}Yb$	$C_{55}H_{40}BCl_6N_{10}Tm$	$C_{108.50}H_{82}B_2N_{20}Nd_2$
fw	1100.16	1309.81	1233.41	1976.04
T/K	193(2)	193(2)	193(2)	193(2)
wavelength/Å	0.71073	0.71073	0.71073	0.71073
cryst syst	triclinic	triclinic	monoclinic	triclinic
space group	$P\bar{1}$	$P\bar{1}$	$P2_1/n$	$P\bar{1}$
a/Å	12.4470(11)	11.9673(5)	18.4931(8)	12.6145(5)
b/Å	14.5765(13)	14.0070(6)	14.6041(6)	13.7314(6)
c/Å	14.6837(13)	20.7721(8)	19.4154(9)	27.843(2)
α/deg	69.585(2)	98.846(2)	90	84.067(2)
β/deg	74.880(2)	100.017(2)	98.808(2)	78.022(2)
γ/deg	89.225(2)	106.862(2)	90	74.461(2)
V/Å^3	2401.5(4)	3203.5(2)	5181.8(4)	4539.5(3)
Z	2	2	4	2
D(calcd) Mg/m^3	1.521	1.359	1.581	1.446

Table 2. Selected Structural Data for Ln(TPP) Complexes[a]

	M−N_{porph} (av)	M−N_{Tp} (av)	M−N_{4plane}[b]	M−N_{3plane}[c]
Yb(TPP)(Tp)	2.348(5)	2.514(9)	1.156(3)	1.796(6)
Tm(TPP)(Tp)	2.364(11)	2.501(2)	1.187(1)	1.782(8)
Nd(TPP)(Tp)	2.438(17)	2.602(8)	1.302(4)	1.891(7)
Nd(TPP)I(THF)$_2$	2.436(16)		1.286(6)	

[a] All measurements in ångstroms. [b] Distance from the metal atom to the least squares plane defined by the four TPP N atoms. [c] Distance from the metal atom to the plane defined by the three coordinated Tp N atoms.

prism being composed of three of the porphyrin N atoms and the three ligating atoms of the remaining ligands, with the final porphyrin N atom comprising the capping group. As shown in Table 2, the metal−ligand distances vary according to the size of the metal ions with Yb and Tm having essentially the same ionic radii while Nd is *ca.* 0.1 Å larger. Because the metal ions do not fit into the cavity of the porphyrin, the porphryin ring adopts a domed conformation to maximize the Ln−N interactions. The structures of the Ln(TPP)Tp complexes confirm the notion that the Tp ligand provides a sterically congested environment around the metal center that should mimimize interactions between the metal and solvent that could reduce the quantum yields for luminescence.

NMR Spectroscopy. A combination of 1-D and 2-D proton NMR techniques were used to characterize the complexes in solution. In all cases, the spectra are consistent with mononuclear structures that have the metal ion sandwiched between the porphyrin ligand and the capping Tp or L(OEt) ligands, as is observed in the solid state. Uncertainty about the magnitude of the contact and pseudocontact shift in new paramagnetic complexes inhibits the a priori assignment of their NMR spectra, but by utilizing the relative integration of the peaks in the one-dimensional proton spectrum coupled with simple two-dimensional experiments, the spectrum can be assigned to the correct protons in the structure.[27] While this provides limited predictive power, it affords the researcher a tool for the rapid analysis of the purity of a previously characterized material, and the ability to determine if a new material has the expected structure.

(27) (a) Luchinat, C. *Coord. Chem. Rev.* **1996**, *150*, 185. (b) Bertini, I.; Coutsolelos, A.; Dikiy, A.; Spyroulias, G. A.; Troganis, A. *Inorg. Chem.* **1996**, *35*, 6308. (c) Spyroulias, G. A.; Coutsolelos, A. G. *Inorg. Chem.* **1996**, *35*, 1382.

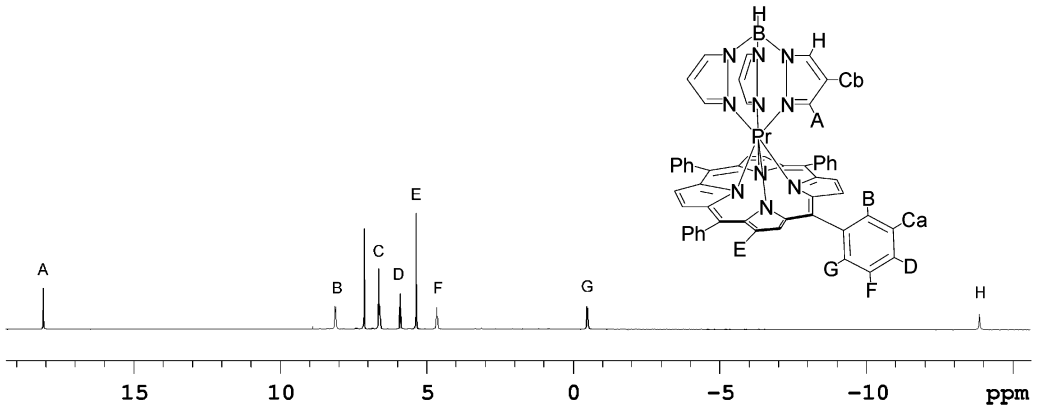

Figure 3. One-dimensional proton NMR spectrum of Pr(TPP)Tp in C_6D_6. The structure with the positions labeled corresponding to the spectrum is presented in the figure.

The one-dimensional proton NMR spectrum of Pr(TPP)-Tp is shown in Figure 3. Assuming the rotation of the phenyl rings on the porphyrin is slow on the NMR time scale,[28] there should be nine proton resonances. Of these nine peaks, five correspond to the protons from the phenyl rings and have an integration of four protons each, three correspond to the Tp protons and have an integration of three protons each, and the ninth peak corresponds to the pyrrole protons and has an integration of eight (the B−H proton is rarely observed even in diamagnetic complexes due to quadrapolar relaxation caused by boron). The spectrum of Pr(TPP)Tp, however, only shows eight peaks with integration ratios of 3:4:7:4:8:4:4:3 (peaks A−H, Figure 3). Variable temperature NMR studies ranging from 40° to 60 °C show that peak C is composed of two overlapping peaks, Ca and Cb, with relative integrations of four and three protons, respectively. Using the integrations, peaks A, Cb, and H are assigned as Tp protons while peaks B, Ca, D, F, and G are assigned to the protons on the phenyl ring and peak E is assigned to the protons on the pyrrole.

In the COSY spectrum of Pr(TPP)Tp (see Supporting Information), there are cross-peaks between A and Cb, and Cb and H, demonstrating that, as expected, those peaks are in the same spin system, consistent with their assignment as Tp ligand protons. Cross-peaks between peaks B and Ca, Ca and D, D and F, and F and G confirm their assignment as phenyl ring protons with peaks B and G being the *ortho* protons, peaks Ca and F being the *meta* protons, and peak D being the *para* proton. Similar experiments on the other new compounds were used to generate the peak assignments that are reported in the Experimental Section of the paper.

Photophysical Properties. Our interest in Ln porphyrin complexes is focused on their application as near-IR emitters in organic light emitting diodes. Each of the lanthanides used in the course of the present synthetic investigation is known to exhibit one or more spectrally narrow emission bands in the 800−1600 nm region in the near-IR. Indeed, we and others have already reported near-IR electroluminescence from devices that contain Yb, Nd, and Er.[2] Thus, to provide a clear understanding of the photophysics and luminescence properties of the new series of Ln porphyrins, each of the complexes was characterized by absorption and room temperature photoluminescence spectroscopy in CH_2Cl_2 solution. In addition, nanosecond time-resolved absorption spectroscopy was carried out on selected complexes in an effort to characterize the nature of the luminescent excited states.

A number of groups have previously characterized the photophysics of Ln porphyrin complexes.[29−34] However, in most cases, due to synthetic limitations, studies of a specific porphyrin ring system were limited to only a few lanthanides and/or capping ligands. Nonetheless, the previous work has revealed a number of important photophysical properties that are characteristic of Ln porphyrins. First, Ln porphyrins display absorption spectra that are typical for "regular metalloporphyrins" (this terminology is derived from Gouterman's original review of the field).[35] Specifically, they feature an intense B (Soret) band near 425 nm due to the allowed $S_0 \rightarrow S_2$ transition, and two weaker Q-bands (Q(1,0) and Q(0,0)) in the 550−600 nm region arising from the orbitally forbidden $S_0 \rightarrow S_1$ transition.[29,35] Porphyrin complexes that contain Yb^{3+}, Er^{3+}, Nd^{3+}, Ho^{3+}, Pr^{3+}, and Tm^{3+} typically display only weak fluorescence and/or phosphorescence in the visible region. This is because the Ln ions introduce a manifold of low-lying f-states which rapidly

(28) Slow rotation of the phenyl rings on the NMR time scale is expected because it has been previously reported in ref 16.

(29) Gouterman, M.; Schumaker, C. D.; Srivastava, T. S.; Yonetani, T. *Chem. Phys. Lett.* **1976**, *40*, 456.
(30) (a) Solovev, K. N.; Tsvirko, M. P.; Kachura, T. F. *Opt. Spectrosc.* **1976**, *40*, 391. (b) Pyatosin, V. E.; Tsvirko, M. P.; Solovev, K. N.; Kachura, T. F. *Zh. Prikl. Spektrosk.* **1981**, *35*, 268; *J. Appl. Spectrosc. (Engl. Transl.)* **1982**, 879. (c) Shushkevich, I. K.; Dvornikov, S. S.; Kachura, T. F.; Solovev, K. N. *Zh. Prikl. Spektrosk.* **1981**, *35*, 647; *J. Appl. Spectrosc. (Engl. Transl.)* **1982**, 1109. (d) Tsvirko, M. P.; Solovev, K. N.; Stelmakh, G. F.; Pyatosin, V. E.; Kachura, T. F. *Opt. Spectrosc.* **1981**, *50*, 300. (e) Pyatosin, V. E.; Tsvirko, M. P.; Solovev, K. N.; Kachura, T. F. *Opt. Spectrosc.* **1982**, *52*, 162. (f) Tsvirko, M. P.; Stelmakh, G. F.; Pyatosin, V. E.; Solovev, K. N.; Kachura, T. F.; Piskarskas, A. S.; Gadonas, R. A. *Chem. Phys.* **1986**, *106*, 467.
(31) Kaizu, Y.; Asano, M.; Kobayashi, H. *J. Phys. Chem.* **1986**, *90*, 3906.
(32) Korovin, Y.; Rusakova, N. *Rev. Inorg. Chem.* **2001**, *21*, 299.
(33) (a) Meng, J. X.; Li, K. F.; Yuan, J.; Zhang, L. L.; Wong, W. K.; Cheah, K. W. *Chem. Phys. Lett.* **2000**, *332*, 313. (b) Wong, W.-K.; Hou, A.; Guo, J.; He, H.; Zhang, L.; Wong, W.-Y.; Li, K.-F.; Cheah, K.-W.; Xue, F.; Mak, T. C. W. *J. Chem. Soc., Dalton Trans.* **2001**, 3092.
(34) Asano-Someda, M.; Kaizu, Y. *J. Photochem. Photobiol., A* **2001**, *139*, 161.
(35) Gouterman, M. In *The Porphyrins, Vol. III*; Dolphin, D., Ed.; Academic Press: New York, 1978; Vol. III, pp 1−165.

Table 3. Absorption and Emission Spectral Properties for Ln(TPP)Tp Complexes in CH_2Cl_2

	absorption λ_{max}/nm (log ϵ)				emission		
Ln	B(1,0)	B(0,0)	Q(1,0)	Q(0,0)	vis λ_{em}	NIR λ_{em}	NIR ϕ_{em}
Ho^{3+}	402(4.55)	423(5.69)	552(4.27)	590(3.61)	649, 715		
Pr^{3+}	402(4.87)	425(5.71)	554(4.31)	593(3.86)	652, 717		
Tm^{3+}	402(4.65)	423(5.80)	551(4.43)	588(3.70)	652, 718		
Nd^{3+}	402(4.67)	424(5.74)	553(4.32)	592(3.76)	651, 717	882, 900, 932, 1069, 1111, 1324, 1354	0.0024
Er^{3+}	402(4.68),	422(5.60)	551(4.21)	590(3.63)	653, 717	1485, 1531[a]	0.0009
Yb^{3+}	402(4.85)	421(5.72)	551(4.41)	588(3.77)	652, 718	932, 954, 977, 990, 1002, 1014, 1022, 1037	0.032

[a] Reported λ_{em} may be blue-shifted slightly from true λ_{em} due to falloff in InGaAs detector response for $\lambda > 1550$ nm.

Table 4. Absorption and Emission Spectral Properties for Ln(TPP)(L(OEt)) Complexes in CH_2Cl_2

	absorption λ_{max}/nm (log ϵ)				emission		
Ln	B(1,0)	B(0,0)	Q(1,0)	Q(0,0)	vis λ_{em}	NIR λ_{em}	NIR ϕ_{em}
Ho^{3+}	405(4.63)	427(5.72)	558(4.30)	597(3.85)	614, 656, 717		
Pr^{3+}	409(4.78)	428(5.81)	561(4.32)	600(4.01)	656, 717		
Tm^{3+}	405(4.62)	426(5.71)	557(4.27)	595(3.76)	611, 655, 717		
Nd^{3+}	409(4.69)	429(5.76)	561(4.39)	600(3.93)	655, 718	829, 896, 947, 1069, 113, 1317, 1350, 1429	0.002
Er^{3+}	406(4.68)	427(5.68)	558(4.34)	596(3.79)	611, 655 720,	1480, 1517,1537[a]	0.001
Yb^{3+}	406(4.60)	427(5.73)	559(4.30)	596(3.76)	612, 655, 719	923, 956, 977, 1003, 1023, 1046	0.024

[a] Reported λ_{em} may be blue-shifted slightly from true λ_{em} due to falloff in InGaAs detector response for $\lambda > 1550$ nm.

quench the lowest singlet and triplet states of the porphyrin ring.[29−31] Finally, a few studies have been reported which show that it is possible to use transient absorption spectroscopy to distinguish the porphyrin localized triplet excited state from the lanthanide f-centered excited states.[30b,c,e]

Tables 3 and 4 summarize important features concerning the near UV−vis absorption and vis−NIR photoluminescence of the entire family of complexes. We first focus attention on the absorption spectra. Band maxima and molar absorptivities of the B- and Q-bands for each of the complexes in CH_2Cl_2 solution are listed in the tables. In addition, the absorption spectra of all of the complexes are included in the Supporting Information section. As expected, each of the complexes exhibit the characteristic features of regular metalloporphyrins.[29] Systematic trends in the absorption maxima as a function of the Ln are not seen, however, close inspection of the data reveals that the B- and Q-bands are systematically red-shifted when the capping ligand is changed from Tp to L(OEt). The origin of this effect is unclear, but the fact that the B- and Q-bands are shifted by approximately the same energy suggests that it arises from a slight ground state destabilization in the Tp complex relative to the L(OEt) complex.

All of the Ln porphyrin complexes exhibit weak photoluminescence as several resolved bands in the 600−720 nm region. The band maxima for the visible emissions are tabulated in Tables 3 and 4. Interpretation of the visible emissions observed is rendered difficult due to the fact that it is believed that most of the samples contain a small amount of free base TPP as an impurity. (Under our conditions, free base TPP in CH_2Cl_2 features two fluorescence bands at 648 and 715 nm.) Inspection of the data for the Tp complexes in Table 3 reveals that the only visible emission that is observed arises from the free base TPP impurity. However, the visible emission of the L(OEt) complexes (Table 4) is more complicated, and importantly, in each case a weak emission band is seen at ≈610 nm. This band is believed to be the Q(0,0) fluorescence from the Ln(TPP)(L(OEt)) complexes. The assignment is supported by the fact that excitation spectra obtained while monitoring the 610 nm emission band correspond to the absorption of the respective Ln(TPP)(L(OEt)) complexes. Our results are not unprecedented, as other groups have also reported weak fluorescence from Ln porphyrins. Specifically, in separate reports Gouterman and co-workers[29] and Kobayashi and co-workers[31] document weak Q(0,0) fluorescence from Yb(OEP)acac, Yb(OEP)OH, and Er(TPP)OH (OEP = octaethylporphyrin). Presumably, the fluorescence arises from the lowest $^1\pi,\pi^*$ (Q) state of the porphyrin in competition with intersystem crossing (ISC) to the $^3\pi,\pi^*$ state. The fluorescence is weak because ISC is likely very fast ($k_{ISC} \approx 10^{10}-10^{11}$ s^{-1}) due to strong spin−orbit coupling promoted by the Ln ion.

Emission studies were carried out in the near-IR region (800−1550 nm) on all of the complexes dissolved in CH_2Cl_2 solution. Near-IR emission was observed for Yb^{3+}, Nd^{3+}, and Er^{3+} complexes where the capping ligand is Tp or L(OEt). No emission was observed for Ln = Ho^{3+}, Pr^{3+} or Tm^{3+} in this spectral range. Tables 3 and 4 list the maxima of the emission lines observed for each of the near-IR luminescent complexes, and Figure 4 illustrates emission from the complexes. Quantum efficiencies (ϕ_{em}) were also determined for the luminescence from the emitting complexes, and the values are listed in the tables. First, the lack of near-IR luminescence from Ho^{3+}, Pr^{3+}, and Tm^{3+} complexes in the 800−1550 nm region is not surprising. Each of these ions has a "ladder" of energetically closely spaced states (e.g., separations of 2000−4000 cm^{-1}) that are below the energy of the $^3\pi,\pi^*$ state of the TPP ligand.[36] Because of the close spacing of the states, nonradiative decay

(36) Dieke, G. H. *Spectra and Energy Levels of Rare Earth Ions in Crystals*; Crosswhite, H. M., Crosswhite, H., Eds.; Interscience: New York, 1968.

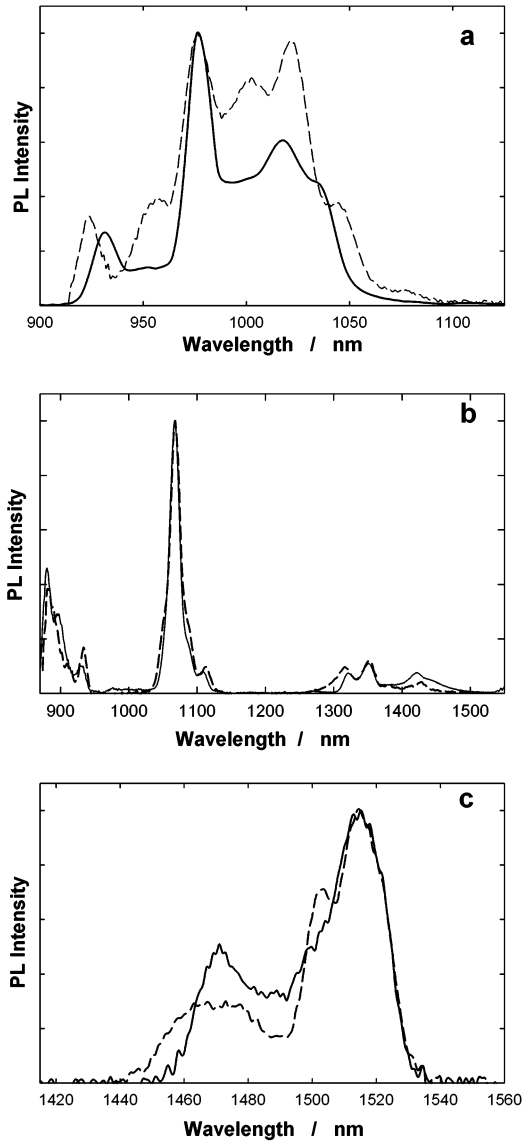

Figure 4. Near-IR photoluminescence spectra of Ln(TPP)L complexes. Solid lines (—), L = Tp, and dashed lines (- - -), L = L(OEt): (a) Yb(TPP)L, (b) Nd(TPP)L, (c) Er(TPP)L.

via coupling to high frequency vibrations (e.g., C−H modes of the ligands and the solvent) is rapid. The emission quantum yields for the luminescent complexes follow the trend $Yb^{3+} > Nd^{3+} > Er^{3+}$, and the yields are not strongly affected by the nature of the capping ligand. The trend in emission quantum yields is consistent with observations on other luminescent lanthanide complexes[1] and reflects the fact that that the efficiency of nonradiative decay increases as the energy of the luminescent state decreases (energy gap law). While the absolute emission quantum yields are comparatively low, they are generally higher than yields of other Yb, Nd, and Er complexes.[1] The enhanced emission yields for the Ln(TPP)Tp and Ln(TPP)(L(OEt)) complexes are believed to arise because the coordination environment provided by the TPP in combination with Tp or L(OEt) effectively shields the Ln ion from interacting with solvent (C−H) vibrational modes which enhance the rate of nonradiative decay. This premise is supported by the observation that ϕ_{em} of Yb(TPP)Tp only increases to 0.034 in $CDCl_3$ (a 7% increase).

The near-IR emission from the Yb^{3+} complexes is shown in Figure 4a. The single transition centered at 977 nm arises from the $^2F_{5/2} \rightarrow {}^2F_{7/2}$ transition,[29,36] and it is split into multiple bands because of splitting by the ligand field.[34] As shown in Figure 4b, the Nd^{3+} complexes feature a rich array of bands in the near-IR region. The luminescence consists of three primary transitions, each of which is split by the ligand field. The transitions are (in order of decreasing energy): $^4F_{3/2} \rightarrow {}^4I_{11/2}$, $^4F_{3/2} \rightarrow {}^4I_{13/2}$, and $^4F_{3/2} \rightarrow {}^4I_{15/2}$.[36] Finally, the Er^{3+} complexes exhibit only one weak emission in the near-IR which corresponds to the $^4I_{13/2} \rightarrow {}^4I_{15/2}$ transition (Figure 4c).[36] The emission is split into two resolved bands presumably due to the ligand field, with the strongest band (1531 nm) exhibiting a shoulder on the short-wavelength side. Interestingly, this shoulder is resolved in Er(TPP)(L(OEt)), where it appears as a resolved band at 1517 nm. This effect apparently reflects the different ligand field presented by the Tp and L(OEt) ligands.

Transient absorption (TA) spectroscopy was carried out on Yb(TPP)Tp, Yb(TPP)(L(OEt)), and Nd(TPP)Tp in order to provide additional information concerning the electronic structure and lifetime of the emitting states. In these experiments, the complexes were excited by a 355 nm laser pulse (10 ns duration, 5 mJ $pulse^{-1}$), and transient absorption difference spectra were recorded at various delay times following the excitation. Figure 5 shows the TA difference spectra for the three complexes over the 450−650 nm region, which coincides with the Q-band ground state absorption bands. In each of the three complexes, weak transient absorption (bleaching) was observed, and the transients decayed with lifetimes of 43, 32, and 44 μs for Yb(TPP)Tp, Yb(TPP)(L(OEt)), and Nd(TPP)Tp, respectively. It is believed that the visible region transient absorption arises from the influence of the *f*−*f* state localized on the lanthanide ion on the porphyrin Q-bands. Consequently, the transient absorption decays provide a measure of the lifetime of the *f*−*f* state, which is also responsible for the near-IR emission. The observed lifetimes are consistent those of other Yb^{3+} and Nd^{3+} complexes that have been previously reported.[1,30]

In each case, the TA spectra are dominated by bleaching of the ground state Q(0,1) and Q(0,0) bands, and increased absorption on the red and blue sides of each Q-band. This pattern of transient absorption was reported in a previous investigation of Yb(TTP) and Yb(etio) (where TTP = 1,5,10,15-tetra-p-tolylporphyrin and etio = etioporphyrin) and was attributed to broadening of the Q-bands caused by the influence of the electronically excited Ln ion.[30b,e] The broadening of the Q-bands may arise for one or more of the following reasons. (1) The excited Ln ion may have a different polarizability, and this may have an influence on the bandwidth of the porphyrin π,π^* transitions. (2) The geometry of the complex may be slightly distorted when the Ln ion is excited, and this may change the geometry of the porphyrin ring. (3) There may be a charge transfer interaction between the porphyrin and the excited state Ln ion which induces broadening of the porphyrin π,π^* transitions.[30b,e]

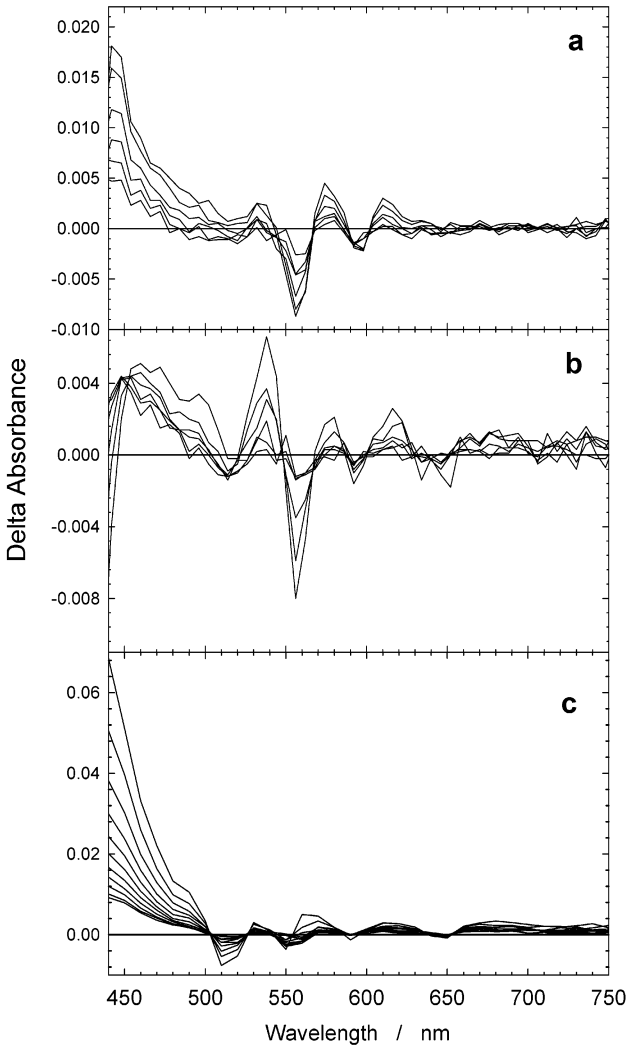

Figure 5. Transient absorption spectra of Ln(TPP)L complexes in CH_2Cl_2 solution. Spectra are obtained at various delay increments following the 355 nm laser excitation pulse, with the first spectrum acquired within 0.5 μs of the excitation: (a) Yb(TPP)(L(OEt)) (8 μs delay increments), (b) Yb(TPP)Tp (8 μs delay increments), (c) Nd(TPP)Tp (16 μs delay increments).

One final point of note is that the TA spectrum of Nd(TPP)Tp features stronger excited state absorption in the region between the Q and B bands (450−500 nm) compared to that of the Yb complexes. Interestingly, this is the region where the TPP-localized $^3\pi,\pi^*$ excited state absorbs strongly.[37] It is possible that in the case of the Nd porphyrin there is an equilibrium population of the TPP-$^3\pi,\pi^*$ produced via thermally activated crossing from the Nd $^4F_{3/2}$ state. Such an equilibrium may be possible because the TPP-$^3\pi,\pi^*$ level is only $\approx$2000 cm^{-1} above the Nd $^4F_{3/2}$ state. The energy gap between the emitting f-state and the TPP-$^3\pi,\pi^*$ level in the Yb^{3+} complexes is >3500 cm^{-1}, and the increased barrier may preclude substantial population of the TPP-$^3\pi,\pi^*$ level to a significant extent. In summary, the TA spectroscopy confirms that in each of the near-IR luminescent complexes the TPP-$^3\pi,\pi^*$ excited state is quenched by the lanthanide ion, and the long-lived states have difference spectra that are consistent with the Ln ion localized f−f state assignment.

Conclusions

A new synthetic method has been developed which facilitates the high-yield and large scale preparation of Ln(TPP) complexes that are capped with various anionic multidentate ligands. The synthesis is demonstrated for a series of 12 complexes, where the lanthanide is Yb, Tm, Ho, Pr, Er, and Nd and the capping ligands are Tp and L(OEt). Each of the complexes is prepared in high yield from a common precursor, Ln(TPP)(X)DME. X-ray structures of three Tp complexes have been obtained, and they are qualitatively similar, with the Ln ion occupying a position that is above the plane defined by the TPP pyrrole nitrogens. The complexes feature absorption spectra that are typical of regular metallophorphyrins, and near-IR photoluminescence is observed for the Yb, Nd, and Er complexes.

In ongoing work, we are exploring the properties of electroluminescent devices fabricated using the Ln(TPP)Tp and Ln(TPP)(L(OEt)) complexes as the active materials. Results of this work will be reported in a forthcoming report.[38]

Acknowledgment. We acknowledge the Army Research Office and the Defense Advanced Research Projects Agency (DAAD19-00-1-0002) for support of this work.

Supporting Information Available: Thermal ellipsoid plots for Yb(TPP)(Tp) and Nd(TPP)(Tp) as well as positional and COSY NMR spectrum for Pr(TPP)Tp, and absorption spectra for all of the Ln(TPP)Tp and Ln(TPP)(L(OEt)) complexes. Crystallographic data in CIF format. This material is available free via the Internet at http://pubs.acs.org.

IC034217G

(37) Tsvirko, M. P.; Sapunov, V. V.; Solovev, K. N. *Opt. Spectrosc.* **1973**, *34*, 635.

(38) Kang, T.-S.; Harrison, B. S.; Foley, T. J.; Knefely, A. S.; Boncella, J. M.; Reynolds, J. R.; Schanze, K. S. *Adv. Mater.* **2003**, *15*, 1093.